5/2016

Front Cover Picture:
R. Raja et al.
Design of Highly Selective Platinum Nanoparticle Catalysts
for the Aerobic Oxidation of KA-Oil using Continuous-Flow Chemistry
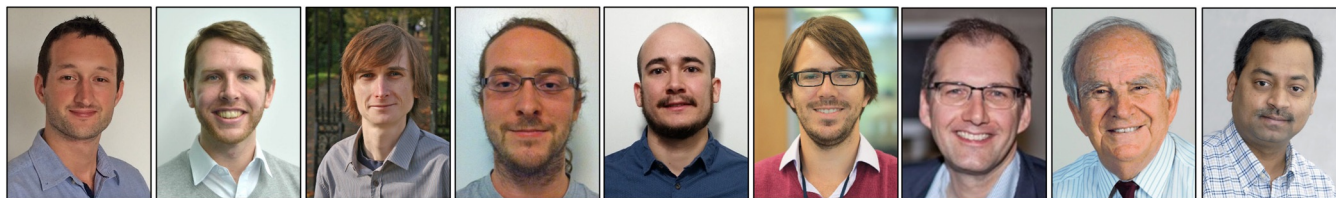
Design of Highly Selective Platinum Nanoparticle Catalysts for the Aerobic Oxidation of KA-Oil using Continuous-Flow Chemistry

Arran Gill   Chris Hinde   Rowan Leary   Matt Potter   Andrea Jouve   Peter Wells   Paul Midgley   John Thomas   Robert Raja

Agency for Science, Technology and Research SINGAPORE   CatalysisHub   UNIVERSITY OF CAMBRIDGE   UNIVERSITY OF Southampton

Invited for this month's cover is the group of Dr. Robert Raja at the University of Southampton, UK. The image shows the origin of spatially isolated and well-defined platinum nanoparticles, within a microporous framework architecture, for the selective aerobic oxidation of KA-oil to cyclohexanone, which is an important precursor in the manufacture of nylon-6. The Communication itself is available at 10.1002/cssc.201501264.

What is the most significant result of this study?

KA-oil is a high-volume industrial feedstock that is generated from the oxidation of cyclohexane. There is considerable industrial interest in selectively converting this to cyclohexanone for the manufacture of adipic acid (nylon-6,6) and ε-caprolactam (nylon-6). Our design approach has revealed that Pt nanoparticles anchored within microporous architectures are effective for the aerobic oxidation of KA-oil using continuous-flow chemistry. The exceptionally high selectivities (99%) and yields (90%) that we have obtained highlight the scientific and industrial merits of our approach when compared with conventional phenol hydrogenation or cyclohexanol dehydrogenation pathways.

When and how did you realize the significance of your findings?

As with most important discoveries, this one originated at the Royal Oak, which is an ancient English Pub in Winchester and supposedly one of the oldest bars in England (1630)! Our industrial collaborators from the USA (Dr. Alan Levy and Dr Scott Keenan from Honeywell) were visiting us and highlighted the potential benefits of having a continuous process for the conversion of KA-oil to cyclohexanone. We were up to the challenge (thanks to Matt, Arran, and Chris) and came up with this patented approach (see Ref. [6]), which is highlighted within this Communication.

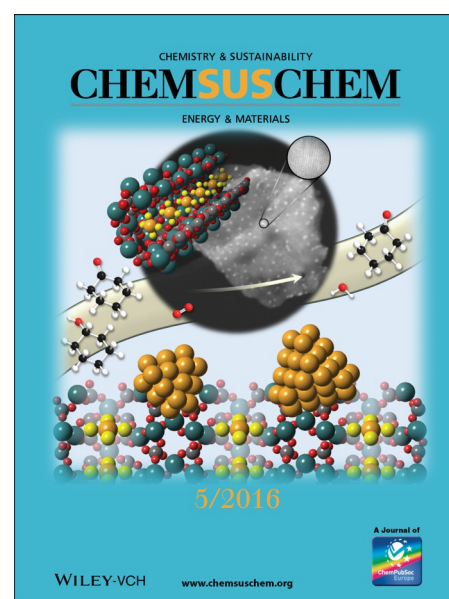## What was the inspiration for this cover picture?

The intricacy and elegance of the catalyst design! The catalysts are produced through a single-step in situ methodology, whereby highly crystalline and isolated metal nanoparticles are thermally extruded from within a three-dimensional porous molecular architecture. This coupled with the utilization of a continuous-flow setup for the aerobic oxidation of KA-oil led to the creation of this Front Cover image.

What other research topics are you working on at the moment?

Our current research efforts are focused on understanding the atomic and molecular basis of catalytic action by porous inorganic solids, based on a detailed structural understanding of the nature of the active sites and their mode of activation. We are working on applications that address fundamental challenges in the chemical, environmental, and photonics landscape, with particular emphasis on sustainable catalysis and renewable energy generation.

Collaborations and Acknowledgement

CHEMISTRY & SUSTAINABILITY

CHEMSUSCHEM

ENERGY & MATERIALS

5/2016

WILEY-VCH   www.chemsuschem.org

Design of Highly Selective Platinum Nanoparticle Catalysts for the Aerobic Oxidation of KA-Oil using Continuous-Flow Chemistry

Arran M. Gill,[a] Christopher S. Hinde,[a] Rowan K. Leary,[b] Matthew E. Potter,[a, c] Andrea Jouve,[a, d] Peter P. Wells,[e, f] Paul A. Midgley,[b] John M. Thomas,[b] and Robert Raja*[a]

Highly active and selective aerobic oxidation of KA-oil to cyclohexanone (precursor for adipic acid and ε-caprolactam) has been achieved in high yields using continuous-flow chemistry by utilizing uncapped noble-metal (Au, Pt & Pd) nanoparticle catalysts. These are prepared using a one-step in situ methodology, within three-dimensional porous molecular architectures, to afford robust heterogeneous catalysts. Detailed spectroscopic characterization of the nature of the active sites at the molecular level, coupled with aberration-corrected scanning transmission electron microscopy, reveals that the synthetic methodology and associated activation procedures play a vital role in regulating the morphology, shape and size of the metal nanoparticles. These active centers have a profound influence on the activation of molecular oxygen for selective catalytic oxidations.

Cyclohexanone is an important commodity chemical used in the production of adipic acid and ε-caprolactam, which are essential precursors used in the industrial manufacture of nylon-6,6 and nylon-6, respectively.[1] The selective hydrogenation of phenol,[2] direct oxidation of cyclohexane[3] and dehydrogenation of cyclohexanol[4] are commonly used for the production of cyclohexanone, either in its pure form or as KA-oil (a mixture of cyclohexanol and cyclohexanone). Given the challenges associated with the aerobic oxidation of hydrocarbons[5] using heterogeneous catalysts, dehydrogenation of cyclohexanol or

KA-oil has proved commercially attractive.[4] In this Communication, we explore the prospects for the aerobic oxidation of KA-oil using heterogenised metal nanoparticle (NP) catalysts (Figure 1). In particular, we have focused on developing a continuous-flow system[6] that would enhance the current yields obtained by the dehydrogenation route whilst at the same time maximizing the overall selectivity (>99%) to the desired cyclohexanone product.
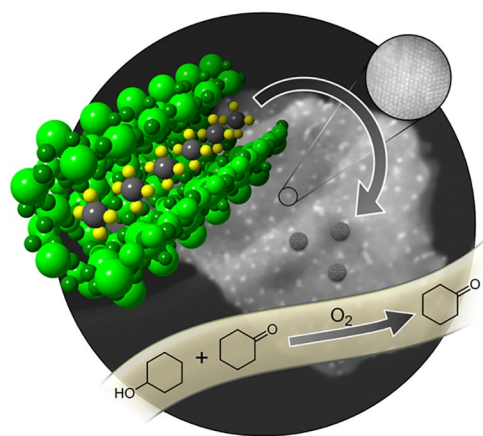

Figure 1. Graphical illustration of the microporous framework architecture containing precursor complexes, which result in well-dispersed and isolated metallic NPs upon activation (as visualized by AC-STEM) that are highly active and selective for the aerobic oxidation of KA-oil.

Noble-metal NPs, including Pt, Pd and Au, have demonstrated a precedent for exceptional activity in a number of selective oxidation and hydrogenation processes.[7] Interestingly, the use of metal NPs in the oxidation of cyclohexanol (and KA-oil in particular) under continuous-flow conditions is somewhat limited (see Table SI 1 a in the Supporting Information). Au/Cu-fiber NP catalysts[8] produce modest cyclohexanone yields (≅75%) but require a complex and intensive catalyst synthesis procedure. A range of Cu-based catalysts[4c,d,9] and other transition-metal variants employing Ti, Co and Mn[10] active centers have been investigated, notwithstanding the fact that a large proportion of these catalysts require high concentrations of corrosive initiators, co-solvents and stoichiometric oxidants. Table SI 1 a highlights some relevant examples of cyclohexanol oxidation and dehydrogenation. It further demonstrates the limited use of continuous-flow methods, with a large majority of catalytic processes utilizing a batch set-up. Developing low-

[a] A. M. Gill, Dr. C. S. Hinde, Dr. M. E. Potter, A. Jouve, Dr. R. Raja
University of Southampton
Southampton, SO17 1BJ (UK)
E-mail: R.Raja@soton.ac.uk

[b] Dr. R. K. Leary, Prof. P. A. Midgley, Prof. J. M. Thomas
University of Cambridge
Cambridge, CB3 0FS (UK)

[c] Dr. M. E. Potter
Georgia Institute of Technology
Atlanta, 30332-0100 (USA)

[d] A. Jouve
University of Turin
Via P. Giuria 7, 10125, Turin (Italy)

[e] Dr. P. P. Wells
UK Catalysis Hub
Oxford, OX11 0FA (UK)

[f] Dr. P. P. Wells
University College London
London, WC1H 0AJ (UK)

Supporting Information for this article is available on the WWW under http://dx.doi.org/10.1002/cssc.201501264.

temperature, selective oxidation of KA-oil could therefore be potentially attractive if cyclohexanone selectivities and yields can rival traditional cyclohexanol oxidation and dehydrogenation pathways.[3,4]

In this study, we capitalize[11] on exploiting the synergistic potential of microporous copper chlorophosphate (CuClP) frameworks bearing flexible anion-exchange properties and devising new synthetic strategies for generating (for a full description, see SI2 in the Supporting Information) in situ isolated and well-defined NPs of Pt, Pd and Au (2–5 nm), as embodied in Figure 1. In particular, changes in the local structural environment of the NPs were monitored over a range of activation temperatures using X-ray absorption spectroscopy (XAS). The shape and size distribution of the active sites within the microporous support architecture were probed using aberration-corrected scanning transmission electron microscopy (AC-STEM), and the compositional integrity of the NPs was ascertained using complementary energy-dispersive X-ray spectroscopy (STEM-EDXS). The findings from here have been rationalized with a view to evaluating structure–property relationships in catalytic studies involving the activation of molecular oxygen. The stability of these solid NPs and versatility of this approach has been investigated in the aerobic oxidation of KA-oil, under continuous-flow conditions, thereby affording potential scope for the industrial applicability of these catalysts.[6]

X-ray photoelectron spectroscopy (XPS) was employed to probe the nature of noble metal species adjacent to the surface of the microporous framework with respect to different activation temperatures (Figures 2a and SI3). A clear trend was observed for the Pt/CuClP catalyst, which showed a transition from a mixture of Pt[II] and Pt[0] with $4f_{7/2}$ peaks at 72.4 and 70.8 eV, respectively, to purely Pt[0] species as the activation temperature was progressively increased from 150 to 200 °C (Figure 2a). Furthermore, it was established that an activation temperature of 200 °C was sufficient for the complete reduc-

tion of the Pt precursors to form NPs under these activation conditions.

XAS was used to probe the coordination geometry and local structural environment of the active sites with a view to gaining a better understanding on NP formation and extrusion with progressive increase in activation temperatures. Concurrent trends with XPS are exhibited in both the EXAFS (extended X-ray absorption fine structure) (Figure 2b) and XANES (X-ray absorption near edge structure) (Figure SI4a) data of the Pt/CuClP material, with evident progressive reduction of the $[PtCl_4]^{2-}$ precursor species across the bulk of the sample. Figure 2b demonstrates the significant decrease in contribution from Pt–Cl neighboring atoms with a concurrent increase in Pt–Pt neighbors as a function of activation temperature. Analogously, due to the direct relationship between the white-line intensity of the L_3-edge and the number of unoccupied Pt 5d states, the diminishing white-line energies displayed in Figure SI4a suggest that the Pt species are approaching the metallic state with progressive increase in activation temperature. In addition, Table SI4a shows that Pt–Pt bond lengths remain consistent with that expected of Pt NPs (above 2.4 nm; 2.76 Å)[12] and that the coordination numbers of the first-shell Pt–Pt scattering path are also lower at 9.6(4) than would be expected of bulk Pt metal (i.e., 12).[13] This indicates that an overwhelming majority of the $[PtCl_4]^{2-}$ precursors are reduced to their metallic state with increase in activation temperature as evidenced by the drastic reduction in the average coordination numbers of adjacent Pt atoms around the central Pt species. These observations juxtaposed with those of the Au and Pd systems (SI4b and c in the Supporting Information) highlight the ease of extrusion of $[PtCl_4]^{2-}$ species from the micropores whereas corresponding powder X-ray diffraction (PXRD) data (Figure SI5a, b, and c) confirm the retention of the structural integrity of the surrounding framework architecture. In the case of Pt, it is clear that the presence of discrete precursor
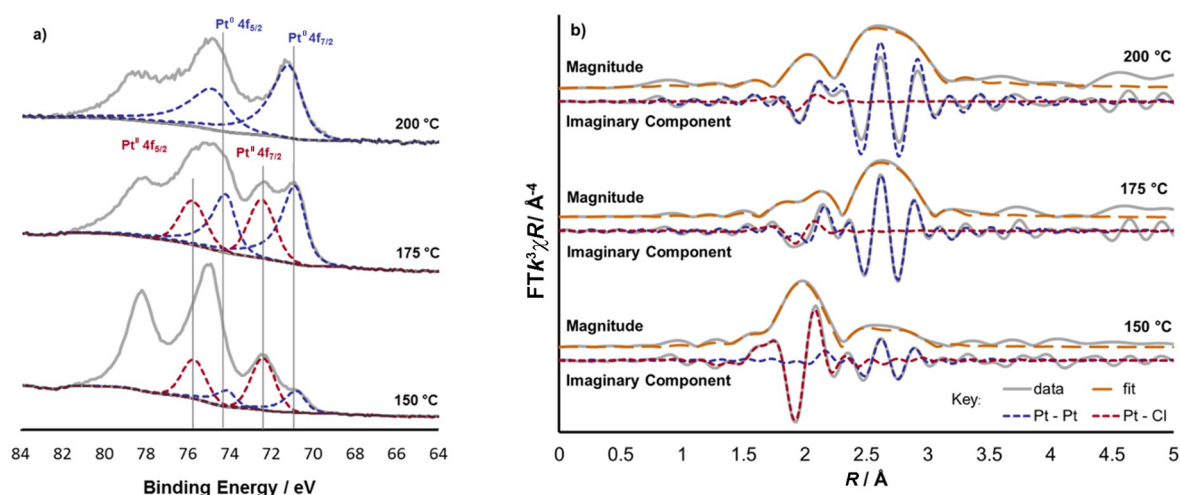

Figure 2. a) XPS spectra (plotted with reference samples in Figure SI3a) and b) magnitude and imaginary component of the k^3-weighted Fourier transform for the EXAFS data (associated scattering paths are included for the imaginary component and the fitting parameters are displayed in Table SI4a) of the three Pt/CuClP species reduced under different activation temperatures. Both techniques demonstrate the progressive reduction of the $[PtCl_4]^{2-}$ precursor towards the metallic Pt[0] species with increase in temperature.

anions within the pores is not detrimental to the overall stability of the microporous framework structure. This is in contrast to that of the Pd/CuClP catalyst (Figure SI5d) where, at temperatures above 200 °C, the structural integrity becomes susceptible to additional phase impurities and degradation of the framework. This could be indicative of stronger interactions between the discrete $[PdCl_4]^{2-}$ anions and the internal pores of the framework, which is currently being investigated.

The Au EXAFS (SI4b in the Supporting Information) emphasizes that the $[AuCl_4]^-$ precursor requires considerably higher activation temperatures[11b] despite the XPS showing surface species with slightly reduced binding energies, characteristic of nanoparticulate Au, being generated above 200 °C (Figure SI3b), which is consistent with earlier work.[14] This suggests that although metallic Au species form on the surface of these materials at 200 °C, higher temperatures and/or alternate activation conditions might be required to achieve extrusions comparable to the Pt catalyst (a detailed study on this is currently underway and only comparable activation conditions are presented here for the sake of consistency). It is well known that $[AuCl_4]^-$ is a non-selective oxidation catalyst,[15] and the low activities observed in our catalytic studies (Figure 3a) with the Au catalyst further vindicates the hypothesis that the adsorbed oxygen species need to be implicated with metallic Au^0 sites for enhanced reactivity.[16]

The catalytic results for the aerobic oxidation of KA-oil using the Pt, Pd and Au catalysts, activated at different temperatures, is presented in Figure 3 (for further details see SI7 in the Supporting Information). Figure 3a highlights the superior performance of the Pt catalyst over that of its corresponding Pd and Au analogues; it is remarkable that the selectivity for the desired cyclohexanone was in excess of 99+% for the Pt catalyst [reaction mixtures were analyzed for dibasic acids (including adipic acid) and we did not observe any evidence for their formation]. Not only is Pt/CuClP a highly effective and selective aerobic oxidation catalyst (the undoped framework is inert, see SI6 in the Supporting Information), but the robust nature of this material is evidenced by both its ability to maintain high levels of activity and selectivity over extended periods on stream, as displayed in Figure 3b (see also Figure SI7a). More

importantly, the material retains its structural integrity post-catalysis as evidenced by both its sustained phase purity (Figure SI5b) and consistent NP size distribution (Figure SI8d), where no agglomeration or restructuring is observed, thus demonstrating the recyclability and stability (Table SI7d) of the catalyst. These findings support the hypothesis that the catalytic activity of these materials can be intrinsically linked to the degree of NP formation: the $[PtCl_4]^{2-}$ precursor has a greater propensity for NP formation over a range of activation temperatures and this, in concert with the surrounding microporous architecture, bestows superior catalytic performance for the aerobic oxidation of KA-oil. To further understand this behavior, all three catalysts were examined using high-resolution STEM, probing the shape and size distribution of the NPs and, in particular, their precise location with respect to the crystalline structure of the microporous framework.

High-resolution studies, using AC-STEM, have shown in detail the abundant formation of nanocrystalline Pt NPs (2–5 nm in diameter), which are well dispersed on the CuClP framework; its crystalline integrity could also be visualized directly (Figures 4a, b and SI8a). In this regard, it is apparent that the atomic number contrast and often 'direct interpretability' of annular dark-field (ADF) STEM imaging, combined with the high-spatial resolution enabled by AC optics, can yield significant insight into the crystallographic structures of both the extruded NPs and the microporous framework. Hence, ADF AC-STEM can be a particularly powerful approach for the elucidation of structure–property relationships in these materials. The much more limited NP formation in the Pd/CuClP system is also readily apparent from AC-STEM as exemplified in Figures 4c and d and SI8b. Complementary compositional studies using STEM–EDXS also confirmed the well-defined nature of the Pt/CuClP and Pd/CuClP systems, with abundance and paucity of NPs, respectively (Figure SI9a and b).

The potentially more complex phenomena in the Au/CuClP system (as seen from the EXAFS data) was also systematically investigated in AC-STEM and STEM-EDXS studies, including samples activated at different temperatures. As shown in Figures 4e and f, SI8c and SI9c, regions of extensive well-defined small NP formation could be observed for the Au/CuClP
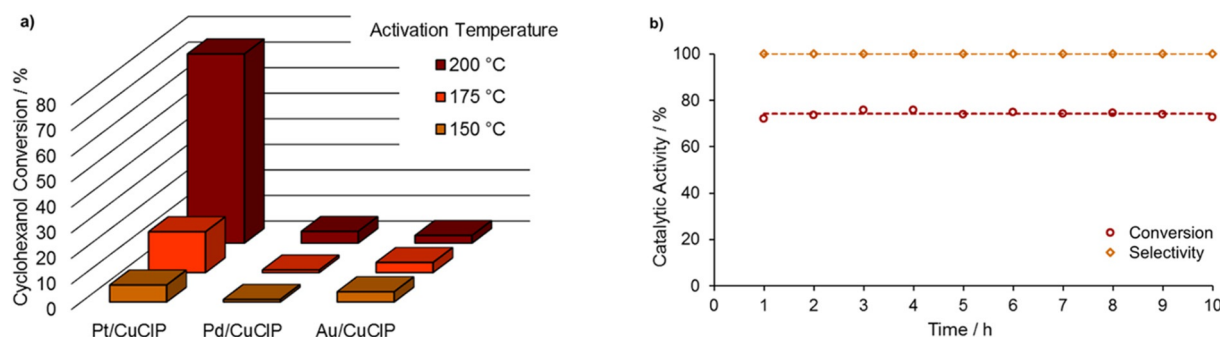

Figure 3. a) Contrasting the aerobic production of cyclohexanone with supported NP/CuClP catalysts, showing the superior activity of Pt/CuClP for this process and the ability to optimize this reaction with adroit catalyst design. b) Highlighting the exceptional catalytic lifetime of the Pt/CuClP catalyst, displaying consistent cyclohexanol conversion and cyclohexanone selectivity profiles over a 10 h period. Full tabulated data is presented in Tables SI7a and b, respectively. Reaction temperature: 200 °C, air flow: 25 mL min^{-1}, substrate flow: 15 µL min^{-1}, weight hourly space velocity (WHSV): 1.8 h^{-1}.
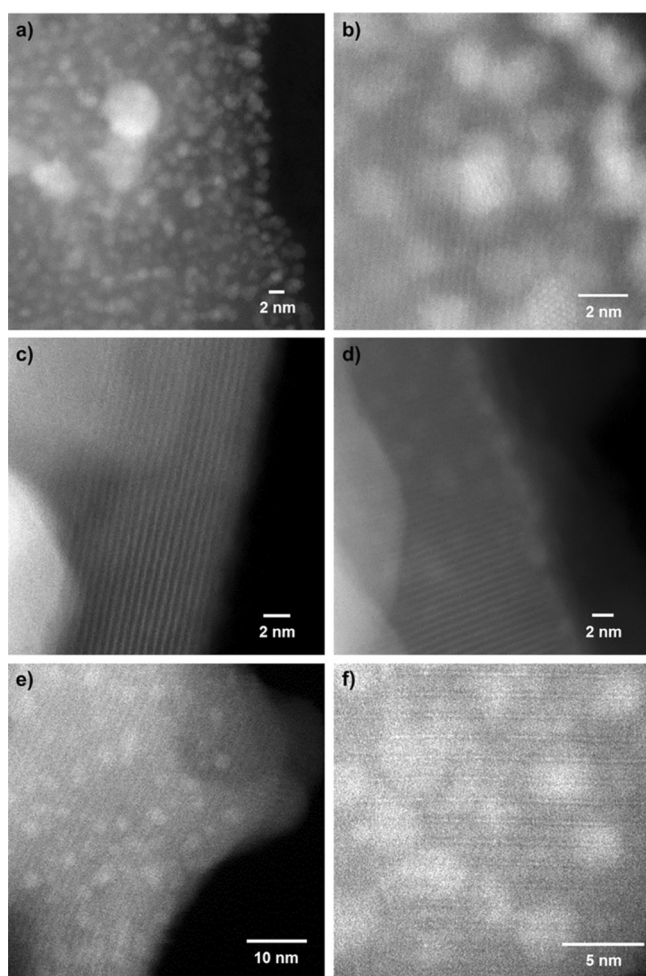
Figure 4. ADF AC-STEM images of the respective NP/CuClP materials activated at 200 °C. The crystalline structure of the framework is rendered visible through the lattice planes containing heavy atoms: a, b) abundance of Pt NPs; c, d) limited Pd NP formation; e, f) prevalence of Au NPs within the CuClP framework. Enlarged figures and further details are provided in SI8 in the Supporting Information.

system, even when the sample was activated at 200 °C (analogous to the Pt/CuClP).

Consistent with the XPS studies, these would appear to predominate at thin or surface regions of the framework. Further, STEM and spatially resolved STEM–EDXS elemental mapping of Au/CuClP samples activated at higher temperatures indicate an increased extrusion of both Au and Cu, with some degree of intermixing. It therefore appears that the Au samples have the potential to possess a range of active species, including small extruded Au NPs on the surface as well as larger Au, Cu or Au–Cu NPs. These preliminary findings therefore indicate the potential for tailored Au/Cu alloying or combined extrusion, which enhances the prospects for exploiting bifunctional (bimetallic) catalysis in the future[7a–d] (these aspects will be reported in detail in a future publication).

By employing a combination of complimentary structural, spectroscopic and high-resolution microscopy techniques, we have contrasted the varying degrees of Pt, Pd and Au NP formation and the superior properties of the $[PtCl_4]^{2-}$ precursor to

yield well-defined, isolated NPs (predominantly 2–3 nm) within microporous framework architectures. The local structural environment, and the precise nature and location of these active sites, is exigent for their superior performance (approaching unrivalled yields of > 90 % by adapting a 'closed-loop' system, Table SI7 d) in the aerobic oxidation of KA-oil under continuous-flow conditions. This design strategy further offers adequate scope for the creation of multi-metallic (e.g., Au–Pt) and multifunctional heterogeneous catalysts in our continued quest for the activation of molecular oxygen in sustainable catalytic processes.[17]

Experimental Section

Details on catalyst synthesis, activation, characterization and catalysis are provided in the Supporting Information. Briefly, the CuClP framework doped with Au, Pt or Pd tetrachloride precursors were hydrothermally synthesized at 448 K for 48 h.[11a] Materials were post-synthetically activated under reduction for 2 h at specified temperatures (423–523 K) under a 150 mL min^{-1} flow of 5 % H_2 in N_2. The aerobic oxidation of KA-oil was studied under continuous-flow conditions under atmospheric pressure employing a custom-made fixed-bed reactor (Cambridge Reactor Design). A typical reaction set-up consisted of 240 mg of catalyst with a substrate flow rate of 15 µL min^{-1} and an air flow rate of 25 mL min^{-1} at 473 K. Products were analyzed and quantified by gas chromatography using appropriate calibrations using 2 M triethyleneglycol dimethyl ether in acetone as external standard.

Acknowledgements

Keywords: aerobic oxidation · flow chemistry · heterogeneous catalysis · nanoparticles · selectivity

[1] a) Cyclohexanol and cyclohexanone: W. B. Fisher, J. F. Van Peppen in *Kirk–Othmer Encyclopedia of Chemical Technology*, Wiley, New York, **2000**, pp. 1–7; b) Cyclohexanol and cyclohexanone: M. T. Musser in *Ullmann's Encyclopedia of Industrial Chemistry*, Wiley-VCH, Weinheim, **2012**, pp. 49–58; c) Oxidation: G. Franz, R. A. Sheldon in *Ullmann's Encyclopedia of Industrial Chemistry*, Wiley-VCH, Weinheim, **2012**, pp. 543–599.

[2] a) H. Liu, T. Jiang, B. Han, S. Liang, Y. Zhou, *Science* **2009**, *326*, 1250–1252; b) J. Scharschmidt, C. Mendoza-Frohn, H. J. Buysch, R. Klotzbucher, (Bayer), US 5395976A, **1995**; c) J. F. Van Peppen, W. B. Fisher, (Allied Chem), US 4092360, **1978**.

[3] a) M. Dugal, G. Sankar, R. Raja, J. M. Thomas, *Angew. Chem. Int. Ed.* **2000**, *39*, 2310–2313; *Angew. Chem.* **2000**, *112*, 2399–2402; b) N. Tani, S. Murata, (Sumitomo Chemical), EP 1350783B1, **2003**.

[4] a) D. R. Cova, (Monsanto), US 2970172, **1961**; b) C. F. Winans, (Wingfoot), US 2218457, **1940**; c) A. Romero, A. Santos, D. Escrig, E. Simon, *Appl. Catal. A* **2011**, *392*, 19–27; d) R. Rao, S. K. Meher, B. G. Mishra, P. H. K. Charan, *Catal. Today* **2012**, *198*, 140–147.

[5] a) G. W. Parshall, S. D. Ittel, *Homogeneous Catalysis: The Applications and Chemistry of Catalysis by Soluble Transition Metal Complexes, 2ⁿᵈ ed.*, Wiley, New York, **1992**; b) J. M. Thomas, R. Raja, G. Sankar, B. F. Johnson, D. W. Lewis, *Chem. Eur. J.* **2001**, *7*, 2972–2978; c) C. L. Hill, *Activation and Functionalization of Alkanes*, Wiley, Chichester, **1989**, Chap. 6–8.

[6] R. Raja, A. B. Levy, S. Keenan, *Nanoparticle catalysts for the conversion of cyclohexanol to cyclohexanone*; application number: US 62235684, filed October 30, **2015**.

[7] a) L. Kesavan, R. Tiruvalam, M. H. A. Rahim, M. I. bin Saiman, D. I. Enache, R. L. Jenkins, N. Dimitratos, J. A. Lopez-Sanchez, S. H. Taylor, D. W. Knight, C. J. Kiely, G. J. Hutchings, *Science* **2011**, *331*, 195–199; b) D. I. Enache, J. K. Edwards, P. Landon, B. Solsona-Espriu, A. F. Carley, A. A. Herzing, M. Watanabe, C. J. Kiely, D. W. Knight, G. J. Hutchings, *Science* **2006**, *311*, 362–365; c) A. B. Hungria, R. Raja, R. D. Adams, B. Captain, J. M. Thomas, P. A. Midgley, V. Golovko, B. F. G. Johnson, *Angew. Chem. Int. Ed.* **2006**, *45*, 4782–4785; *Angew. Chem.* **2006**, *118*, 4900–4903; d) S. Hermans, R. Raja, J. M. Thomas, B. F. G. Johnson, G. Sankar, D. Gleeson, *Angew. Chem. Int. Ed.* **2001**, *40*, 1211–1215; *Angew. Chem.* **2001**, *113*, 1251–1255; e) K. Mori, T. Hara, T. Mizugaki, K. Ebitani, K. Kaneda, *J. Am. Chem. Soc.* **2004**, *126*, 10657–10666; f) A. L. Tarasov, L. M. Kustov, A. A. Bogolyubov, A. S. Kiselyov, V. V. Semenov, *Appl. Catal. A* **2009**, *366*, 227–231.

[8] G. Zhao, H. Hu, M. Deng, M. Ling, Y. Lu, *Green Chem.* **2011**, *13*, 55–58.

[9] B. M. Nagaraja, A. H. Padmasri, P. Seetharamulu, K. H. P. Reddy, B. D. Raju, K. S. R. Rao, *J. Mol. Catal. A* **2007**, *278*, 29–37.

[10] a) A. Corma, P. Esteve, A. Martnez, *J. Catal.* **1996**, *161*, 11–19; b) S. A. Chavan, D. Srinivas, P. Ratnasamy, *J. Catal.* **2002**, *212*, 39–45.

[11] a) C. S. Hinde, S. Van Aswegen, G. Collins, J. D. Holmes, T. S. A. Hor, R. Raja, *Dalton Trans.* **2013**, *42*, 12600–12605; b) C. S. Hinde, D. Ansovini, P. P. Wells, G. Collins, S. Van Aswegen, J. D. Holmes, T. S. A. Hor, R. Raja, *ACS Catal.* **2015**, *5*, 3807–3816.

[12] J. H. Kang, L. D. Menard, R. G. Nuzzo, A. I. Frenkel, *J. Am. Chem. Soc.* **2006**, *128*, 12068–12069.

[13] A. I. Frenkel, C. W. Hills, R. G. Nuzzo, *J. Phys. Chem. B* **2001**, *105*, 12689–12703.

[14] a) J. T. Miller, A. J. Kropf, Y. Zha, J. R. Regalbuto, L. Delannoy, C. Louis, E. Bus, J. A. van Bokhoven, *J. Catal.* **2006**, *240*, 222–234; b) M. Turner, V. B. Golovko, O. P. H. Vaughan, P. Abdulkin, A. Berenguer-Murcia, M. S. Tikhov, B. F. G. Johnson, R. M. Lambert, *Nature* **2008**, *454*, 981–983.

[15] a) B. Pal, P. K. Sen, K. K. S. Gupta, *J. Phys. Org. Chem.* **2001**, *14*, 284–294; b) V. Soni, R. S. Sindal, R. N. Mehrotra, *Polyhedron* **2005**, *24*, 1167–1174.

[16] a) B. Xu, X. Liu, J. Haubrich, R. J. Madix, C. M. Friend, *Angew. Chem. Int. Ed.* **2009**, *48*, 4206–4209; *Angew. Chem.* **2009**, *121*, 4270–4273; b) B. Xu, L. Zhou, R. J. Madix, C. M. Friend, *Angew. Chem. Int. Ed.* **2010**, *49*, 394–398; *Angew. Chem.* **2010**, *122*, 404–408.

[17] M. E. Potter, A. J. Paterson, B. Mishra, S. D. Kelly, S. R. Bare, F. Corà, A. B. Levy, R. Raja, *J. Am. Chem. Soc.* **2015**, *137*, 8534–8540.